Holocene sedimentation in a blue hole surrounded by carbonate tidal flats in The Bahamas: Autogenic versus allogenic processes

Peter J. van Hengstum[a,b,*], Tyler S. Winkler[b], Anne E. Tamalavage[b], Richard M. Sullivan[b], Shawna N. Little[c], Dana MacDonald[d], Jeffrey P. Donnelly[e], Nancy A. Albury[f]

[a] Department of Marine Science, Texas A&M University at Galveston, Galveston, TX 77554, USA
[b] Department of Oceanography, Texas A&M University, College Station, TX 77843, USA
[c] Department of Marine Biology, Texas A&M University at Galveston, Galveston, TX 77554, USA
[d] Department of Geosciences, University of Massachusetts-Amherst, Amherst, MA 01003, USA
[e] Coastal Systems Group, Woods Hole Oceanographic Institution, Woods Hole, MA 02543, USA
[f] National Museum of The Bahamas, PO Box EE-15082, Nassau, the Bahamas

ABSTRACT

The sediment in North Atlantic blue holes preserves paleoclimate records. However, accurate paleoclimate reconstructions require an improved understanding of allogenic versus autogenic processes controlling blue hole sedimentation. Here we provide a detailed case study of the Holocene stratigraphy within Freshwater River Blue Hole, which is currently surrounded by carbonate tidal flats in the northern Bahamas (Abaco Island). During the Holocene, concomitant coastal aquifer elevation and relative sea-level rise controlled internal blue hole depositional environments. The general Holocene facies succession observed is: (i) basal detrital and freshwater peat, (ii) palustrine to lacustrine marl, (iii) algal sapropel, and finally (iv) bedded carbonate mud. During the middle Holocene when groundwater levels were lower, small changes in accommodation space that were inherited from the bedrock surface below (< 1 m) were able to promote significant lateral facies changes. Multiple cores are needed to characterize these lateral facies changes. Hydrographic characteristics of the coastal aquifer (e.g., vertical position, stratification, salinity) relative to the blue hole benthos exert a fundamental control on (a) benthic flora and meiofauna (e.g., charophytes, ostracodes, foraminifera, gastropods) and (b) organic matter production and preservation from pelagic productivity. Over the last 5000 years, water column stratification in Freshwater River Blue Hole was interrupted on millennial to sub-decadal timescales , which are potentially linked to changing aquifer recharge and rainfall. Lastly, historical intense hurricanes passing closely to the west of the site may have promoted deposition of coarse beds at the site. However, the lack of carbonate tidal flat microfaunal remains (foraminifera: *Peneroplis*) within these coarse intervals indicates that Freshwater River Blue Hole does not preserve a reliable record of hurricane-induced overwash deposition from the carbonate tidal flats during the last 2300 years.

1. Introduction

Classic circular-shaped blue holes and sinkholes are common on carbonate platforms in the Tropical North Atlantic Ocean, and they ignited curiosity in Caribbean idifenous people and earliest European Explorers (Agassiz, 1894; Pearse et al., 1936). The colloquial terms blue hole (Bahamas), sinkhole (Florida), and cenote (Mexico) all describe identical karst features that are derived from the same physical process. In short, limestone platforms internally dissolve to create caves during Quaternary sea-level oscillations, and cave ceilings eventually collapse (Cole, 1910; Mylroie et al., 1995). After formation, lake-like blue holes become natural sediment traps that can accumulate scientifically significant paleoenvironmental archives, whose preservation is often enhanced by dysoxic to anoxic groundwater (Hine and Steinmetz, 1984; Shinn et al., 1996). Over the past few decades, blue holes have yielded ecological and climate records spanning the Last Glacial Maximum until present (Grimm et al., 1993; Steadman et al., 2007; Slayton, 2010), Holocene records of aquifer hydrodynamics (Alverez Zarikian et al., 2005; van Hengstum et al., 2010), and paleo tropical cyclone records (Lane et al., 2011; Brandon et al., 2013; van Hengstum et al., 2016). Offshore blue holes also preserve high-resolution tropical cyclone and climate records (Gischler et al., 2008; Denomee et al., 2014; van

---

* Corresponding author at: Department of Marine Science, Texas A&M University at Galveston, Galveston, TX 77554, USA.
 E-mail address: vanhenp@tamug.edu (P.J. van Hengstum).

Hengstum et al., 2014; Wallace et al., 2019), and filled-in blue holes can be observed in seismic reflection surveys (Weij et al., 2019). However, long-term sedimentary processes operating in blue holes remain poorly understood, and uncertainty remains regarding allogenic versus autogenic influences on the preserved stratigraphic architecture. Extracting meaningful paleoclimate records from blue holes first requires a robust understanding of their internal sedimentary dynamics.

A complete Holocene stratigraphic record from a currently submerged blue hole, in either an intertidal or subtidal setting, has yet to be documented. In blue holes on the subaerial landscape, deposition is strongly linked to the physical conditions and biologic activity promoted by the physical conditions of the local coastal aquifer (e.g., salinity, oxygenation) and its constituent water masses (e.g., meteoric lens, mixing zone, saline groundwater). For example, wetlands can develop in intertidal conditions when a blue hole is first flooded by meteoric groundwater, and accumulating plant detritus can create basal peat deposits (Gabriel et al., 2009; Slayton, 2010; Lane et al., 2011). However, not all blue holes have basal peat deposits (van Hengstum et al., 2016; Gregory et al., 2017). As water depth increases from relative sea-level rise, deposition can shift to organic-rich sapropel (van Hengstum et al., 2016; Gregory et al., 2017), detrital peat (Steadman et al., 2007), or palustrine to lacustrine marls (Slayton, 2010; Peros et al., 2017; van Hengstum et al., 2018). Changes in terrestrial vegetation, such as wetland colonization, can also impact local sediment production and deposition in a blue hole (Collins et al., 2015; Gregory et al., 2017; Tamalavage et al., 2018). It is expected that fully marine conditions are initiated when groundwater flooding the blue hole becomes circulated with the ocean through the limestone, either through diffuse, fracture or conduit flow. Several authors have provided conceptual models for environmental, groundwater, and sedimentary changes in blue holes during a transgressive cycle (Shinn et al., 1996; Surić et al., 2005; van Hengstum et al., 2011; Gregory et al., 2017). Most conceptual models depict blue holes as hydrologically open systems that are well-connected to the local groundwater system.

Here we present a detailed analysis of the Holocene infill in Freshwater River Blue Hole in The Bahamas. This site is currently surrounded by carbonate tidal flats in response to recent flooding of the antecedent carbonate landscape by Holocene sea-level rise. The sedimentary record in Freshwater River Blue Hole preserves evidence of: (i) initial wetland conditions generated by concomitant Holocene sea-level and groundwater-level rise, (ii) alternating aquatic conditions caused by the local groundwater column oscillating between stratified and uniform conditions, and finally (iii) the onset of marine-influenced conditions when the surrounding subaerial landscape became flooded by sea-level rise and transitioned into carbonate tidal flats.

2. Study Site: Freshwater River Blue Hole

The Little Bahama Bank in the Bahamian archipelago consists of Grand Bahama Island and Abaco Island (Fig. 1). The carbonate tidal flats on the western margin of Abaco Island are known locally as "The Marls", which host an economically-significant bonefish industry (*Albula vulpes*, Adams and Cooke, 2016; Sherman et al., 2018). Sediment production on Bahamian carbonate tidal flats is significant to regional sediment budgets on both the shallow carbonate platform and proximal deep-sea areas (Neumann and Land, 1975). However, the geological framework for the carbonate tidal flats on western Abaco Island (e.g., sedimentary processes, subsurface stratigraphy, and emplacement age) remain poorly understood when compared to carbonate tidal flats in northern Andros (Shinn et al., 1969; Maloof and Grotzinger, 2012), Crooked Island (Berkeley and Rankey, 2012) and North Caicos Island (Tedesco and Aller, 1997). Elsewhere in the Bahamian archipelago, the Holocene sediment thickness on carbonate tidal flats is generally < 2 m, and vertically mixed by bioturbation and local hydrodynamics.

An enclosed area near the western Abaco shoreline is colloquially referred to as 'The Freshwater River' (Fig. 1), which contains several

nearby blue holes including Meredith's Blue Hole (26.3945° N, −77.1691° W), Centerville Blue Hole (26.413°N, −77.218° W), Steve's Cay Blue Hole (26.478° N, −77.180° W), and Freshwater River Blue Hole (26.426° N, −77.175° W). Freshwater River Blue Hole is oblong shaped (roughly 90 m by 60 m), and 5 to 15 m in depth. The blue hole is surrounded by 50 to 100 m of supratidal island colonized by juvenile red and white mangrove, with mature trees forming a more wooded area in the southwest (Fig. 2).

Subsurface lithology on the Little Bahama Bank is characterized by an uppermost ~15–30 m thick Pleistocene limestone resting on dolomite below (Kaldi and Gidman, 1982; Melim and Masaferro, 1997; Whitaker and Smart, 1997). Kindler and Hearty (1997) reviewed Bahamian stratigraphy exposed in outcrop and its relationship to Pleistocene sea-level oscillations, but a similar approach has not yet been extended to subsurface stratigraphy. In southern Abaco at Borehole 61, Kaldi and Gidman (1982) describe a dolomite unit (47 to ~25 m total well depth), a ~6 m calcrete unit that is thought to reflect subaerial exposure (~25 to 18 m total well depth), and the uppermost limestone unit (0 to ~18 m total well depth, identified as the Lucayan Formation by original authors). No significant lithological variability (e.g., paleosol horizons, laterite) was noted in the uppermost 18 m thick limestone at Borehole 61 in southern Abaco (Kaldi and Gidman, 1982). In a N-S transect spanning the western Little Bahama Bank over Grand Bahama, the upper limestone unit has a nearly uniform thickness of ~20 m (Vahrenkamp et al., 1991; see fig. 2 in Vahrenkamp and Swart, 1994). In the recent climate (~1850 to 2017, Common Era), the northern Bahamas including the Little Bahama Bank experienced a mean annual rainfall of ~1450 mm/yr (Jury et al., 2007).

The Holocene flooding history of the Little Bahama Bank is critical for understanding the regional landscape change and subsurface hydrogeology. The Bight of Abaco is a shallow carbonate lagoon (currently < 9 m depth) separating Grand Bahama Island and Abaco Island (Fig. 1B), and this area has been important for understanding carbonate platform sediment production, transport, and export to the deep-sea on glacial to interglacial timescales (Neumann and Land, 1975; Droxler et al., 1983; Pilskan et al., 1989; Reeder and Rankey, 2009; Slowey and Henderson, 2011; Fauquembergue et al., 2018). The Holocene environmental succession in the Bight of Abaco, and its preserved stratigraphic record, are similar to other carbonate platforms with central depressions (Ashmore and Leatherman, 1984; see Fig. 6 in Pilskan et al., 1989; Mackinnon and Jones, 2001). By re-calibrating the conventional radiocarbon ages from (Rasmussen et al., 1990) with IntCal13 (Reimer et al., 2013), the deepest areas in the Bight of Abaco (10.87 m below sea level, mbsl) transitioned from a terrestrial landscape into a freshwater environment ~8790 years ago (median probability calibration result). The modern marine lagoon became established when a bedrock sill at ~3.7 mbsl between Grand Bahama and Moore's Island was flooded by Holocene sea-level rise and initiated seawater exchange between the Bight of Abaco and the Northwest Providence Channel (Rasmussen et al., 1990). The timing for when this sill was flooded depends upon the radiocarbon calibration curve used (Reimer et al., 2013) to calibrate the marine bivalve *Anodontia alba* from Rasmussen et al. (1990): either (a) it occurred at ~5570 years ago (median probability result with IntCal13), or (b) ~5985 years ago (median probability result with Marine13) (Reimer et al., 2013). The older age of ~5985 is within dating uncertainties for onset of the main growth (6500 ± 900 cal yrs BP to present) of the offshore Holocene carbonate wedge on the northern slope of Little Bahama Bank (Fauquembergue et al., 2018). It is thought that the shallow carbonate lagoons on the Little Bahama Bank, like the Bight of Abaco, are the sediment source for this carbonate wedge (Fauquembergue et al., 2018).

3. Methods

The bathymetry of Freshwater River Blue Hole was mapped with a 200/30 kHz dual channel HydroLite-DFX echosounder (± 0.01 m
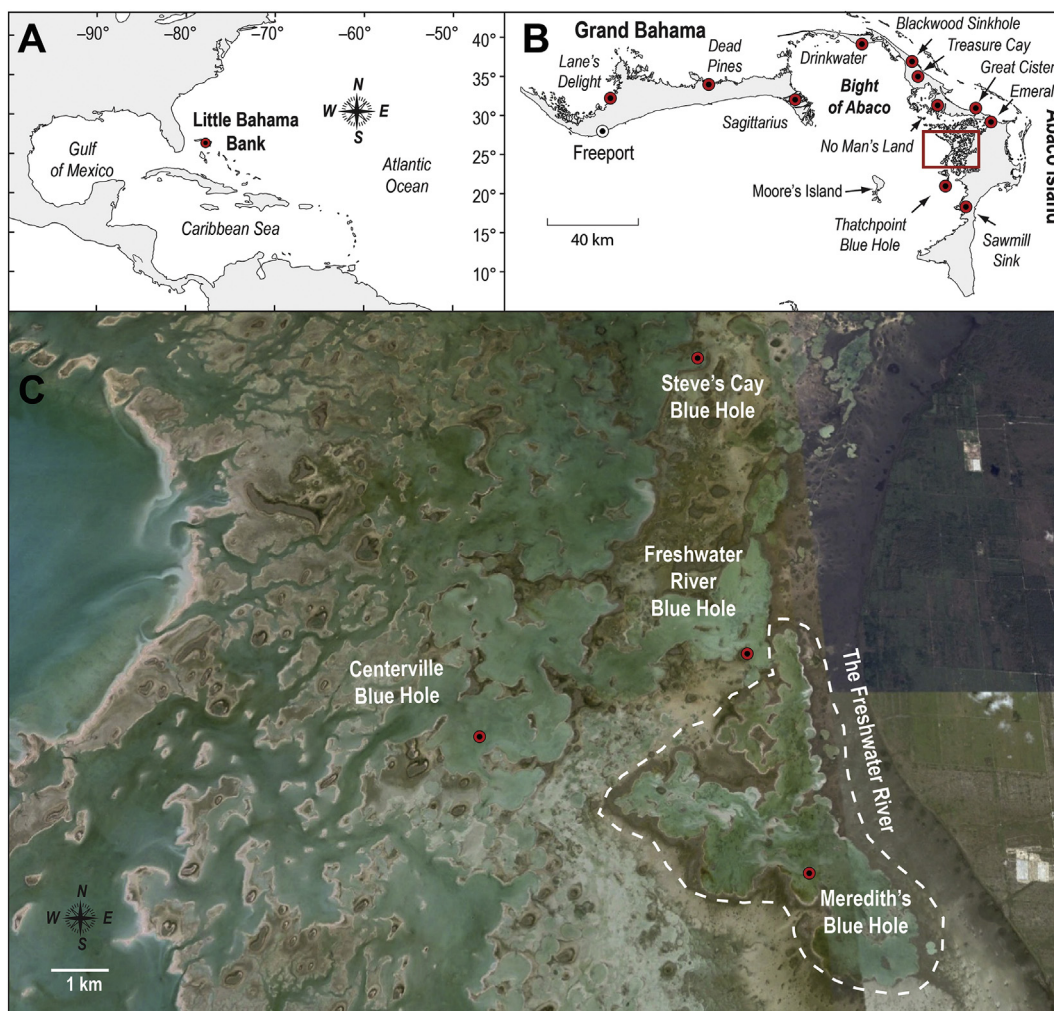
Fig. 1. (**A**) The Little Bahama Bank lies in the Northern Bahamas, east of Florida. (**B**) Locations of several blue holes and sinkholes on the Little Bahama Bank, including No Man's Land (van Hengstum et al., 2018), Emerald Pond (Slayton, 2010), Sawmill Sink (Steadman et al., 2007). (**C**) True color photograph of carbonate tidal flats in Abaco, and the area referred locally to 'The Freshwater River' is outlined in a dashed line. (For interpretation of the references to color in this figure legend, the reader is referred to the web version of this article.)

vertical uncertainty) and a Garmin GPS unit (± 3 m horizontal uncertainty), with final data interpolation in ArcGIS. Depth to the sediment water interface is 5 to 8 m (Fig. 2), but the bathymetry is not a simple bowl shape. In contrast, sediment has preferentially accumulated in the centre rather than the margins. Sediment cores (7.6 cm diameter, Table 1) were collected from Freshwater River in 2014 (push core: FWRBH-C2) and 2016 (Submersible Rossfelder P3 vibracore: FRSH-C2, FRSH-C3). The vibracores all terminated at a hardground and thus sampled the entire unlithified sedimentary sequence (Fig. 2, Table 1). Immediately after coring and while the pipe was still positioned vertically in the water column, floral foam was manually inserted into the core pipe to stabilize the sediment-water interface. This procedure can preserve the integrity of the sediment architecture in the upper 10 cm of the core while long core pipes are subsequently stored and transported horizontally. In the laboratory, sediment cores were split lengthwise, photographed, X-rayed, and stored at 4 °C until further analysis. Sediment terminology for sapropel and peat followed Schnurrenberger et al. (2003).

The variability in the coarse sediment fraction was measured using the Sieve-first Loss-on-Ignition procedure (van Hengstum et al., 2016). This technique is well suited for characterizing the variability of the coarse fraction in highly heterogeneous carbonate sediments. Contiguous 1-cm sediment sub-samples, with a standardized initial volume of 2.5 cm^3, were *first* wet sieved over a 63-μm mesh, dried for 12 h in an oven at 80 °C and weighed to determine the original sediment mass. Samples were then combusted for 4.5 h at 550 °C in a muffle furnace to remove sedimentary organic matter, as per experiments of Heiri et al. (2001), and re-weighed to determine mineral mass remaining after combustion. The variability in coarse sediment was then expressed as mass per unit volume ($D_{>63μm}$ mg cm^{-3}). A value of $D_{>63μm}$ equal to 0 mg cm^{-3} would indicate that no sand-sized or greater sediment particles were present at that stratigraphic level (e.g., foraminifera, peloids, shells, ooids). For the uppermost bedded carbonate mud unit in FRSH-C3, additional sediment sub-samples were sieved over a 63 μm mesh from the coarsest horizons (12–13 cm, 20–21 cm, 66–67 cm, 78–79 cm) and finest horizons (9–10 cm, 57–58 cm, 130–131 cm) for further stereomicroscopic examination. Coarse sediment was examined wet in Petri dishes to investigate the provenance of coarse sedimentary particles and shells. Finally, new sediment sub-samples were obtained at contiguous 1-cm intervals down core and subjected to a Classic LOI procedure to determine variation in bulk organic matter content, as per standard methods (550 °C for 4.5 h) (Dean Jr, 1974; Heiri et al., 2001). Uncertainty on replicate Classic LOI samples is typically less than ± 1%.

Representative sediment samples from each sedimentary unit were examined for meiofaunal and botanical remains (e.g., testate amoebae, benthic foraminifera, ostracodes, achenes, seeds, and charophytes) to investigate water column salinity and oxygen changes through time.
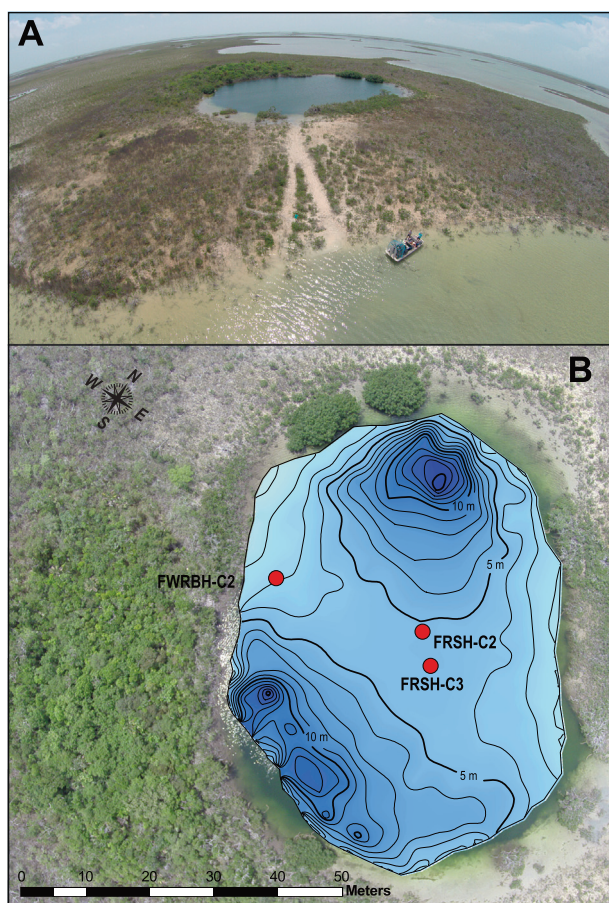
Fig. 2. (A) Aerial photograph of Freshwater River Blue Hole facing to the west. (B) Aerial photograph of Freshwater River Blue Hole overlain by the bathymetry and core sites. Photographs were collected with a DJI Phantom drone equipped with a GoPro camera (Pete van Hengstum). (For interpretation of the references to color in this figure legend, the reader is referred to the web version of this article.)

Multiple sub-samples from the primary lithologies were wet-sieved over a 63-μm mesh, with the remaining coarse sediment residue examined under a stereomicroscope. Observed meiofaunal remains include ostracodes and calcareous foraminifera, but not freshwater testate amoebae (e.g., *Centropyxis aculeata*) or agglutinated foraminifera (e.g., *Trochammina inflata* or *Entzia macrescens*). Representative specimens were imaged by scanning electron microscopy (SEM) on a Hitachi Desktop SEM, and taxonomy followed available regional and international resources (Loeblich Jr. and Tappan, 1987; Teeter, 1989; van Hengstum et al., 2018). In addition, FRSH-C3 was contiguously sub-sampled (2.5 cm³) downcore at 1 cm intervals and washed over a 125 μm mesh to specifically examine charophyte remains. Vegetation nomenclature follows Correll and Correll (1982).

Age control was established by radiocarbon dating of samples (*n* = 40) at the National Ocean Sciences Accelerator Mass Spectrometry at Woods Hole Oceanographic Institution (**Appendix 1**). Only

terrestrial plant macrofossils (e.g., twigs, leaves) were dated to avoid challenges from the hard water effect (e.g., aquatic organic matter, shells). Radiocarbon dates were strategically concentrated in FRSH-C3, the most complete sequence recovered. All conventional radiocarbon age results were calibrated to calendar years before present (cal yr BP) with IntCAL13 (**Appendix 1**), whereby 1950 Common Era (CE) is considered present (Reimer et al., 2013). However, one date returned a $F^{14}C$ value > 1 (FRSH-C3-9.5 cm depth, **Appendix 1**) that indicates that the plant tissue is younger than 1950 CE and was calibrated with CaliBOMB (Hua and Barbetti, 2004). Bayesian age-depth modelling analysis indicates that the lower probability 2σ calibrated result of 1958 CE is more likely to be accurate, given it produces consistent sedimentation rates over the last millennium, and there are no stratigraphic indicators in FRSH-C3 that suggest a change in sedimentary rate (e.g., erosion) in the last century. Final sedimentation rate and a down core age model for FRSH-C3 were computed using the R program *Bacon v2.2* (Blaauw and Christen, 2011).

Holocene environmental change in Freshwater River Blue Hole was compared to relative sea-level rise using the Bahamian sea-level curve of Khan et al. (2017), and a simple model to illustrate water level change inside the blue hole. This model assumes that the depth to the limestone at the core site of FRSH-C3 is the deepest part of the blue hole, it ignores sediment accumulation in the blue hole through time, and it assumes that the groundwater level in the blue hole and relative sea-level are at the same elevation (negligible regional hydraulic gradient). Although simple, this model permits a first-order assessment of changes in groundwater level and the maximum potential water column depth in the Freshwater River Blue Hole through time.

4. Sedimentary facies and chronology

4.1. Blue hole flooding and peat deposition: 8300 to ~7600 cal yrs BP

Peat is at the base of the vibracores, which can be divided into two layers based on the general size of the constituent organic matter particles (Figs. 3, 4): a fragmental granular peat (freshwater peat) vs. fragmental herbaceous peat (detrital deat). A ~10 cm thick unit of fragmental herbaceous peat (plant fragments: > 2 mm) occurs at the base of FRSH-C2 and FRSH-C3 that began accumulating by ~8360 ± 30 cal yrs BP in FRSH-C3. The plant fragments in the fragmental herbaceous peat were notably larger, and slightly darker in color than the fragmental granular peat unit above. The fragmental herbaceous peat had a mean bulk organic matter content of 76 ± 1% (Fig. 5, range: 75–79%, *n* = 11), and relatively low amounts of coarse mineral matter (mean $D_{>63um}$: 2.1 ± 0.4 mg/cm³, range 1.7 to 3.1 mg/cm³, *n* = 11).

Deposition of fragmental granular peat (plant fragments: 0.1 to 2 mm) began at ~8170 ± 25 cal yrs BP. This layer had a similar, but more variable bulk organic matter content than the fragmental herbaceous peat (mean 70 ± 1%, range: 19 to 80%, *n* = 56). It also had slightly more coarse-grained mineral content (mean $D_{>63um}$: 6.5 ± 12.3 mg/cm³, range: 0.1 to 54.2 mg/cm³, *n* = 56). The fragmental granular peat contained the ostracodes *Darwinula stevensoni* and *Cypridopsis vidua*, which are both well known from freshwater aquatic environments (Rasmussen et al., 1990; Alverez Zarikian et al., 2005;

Table 1
Core locations, lengths, and location based on the global position system.

Core	Recovery method	Water depth[a] (m)	Reason coring stopped	Length of sampled sediment column (m)	Final compressed core length (cm)	Latitude (°N)	Longitude (°W)
FWRBH-C2	Push	3.8 ± 0.1	Limit of push drive	2.9 ± 0.1	211	26.42611	77.17599
FRSH-C2	Rossfelder P3	4.8 ± 0.1	Hit hardground	3.5 ± 0.1	322	26.42615	77.17574
FRSH-C3	Rossfelder P3	4.9 ± 0.1	Hit hardground	4.0 ± 0.1	370	26.4261	77.1757

[a] Water depth derived from HydroLite-DFX echosounder.
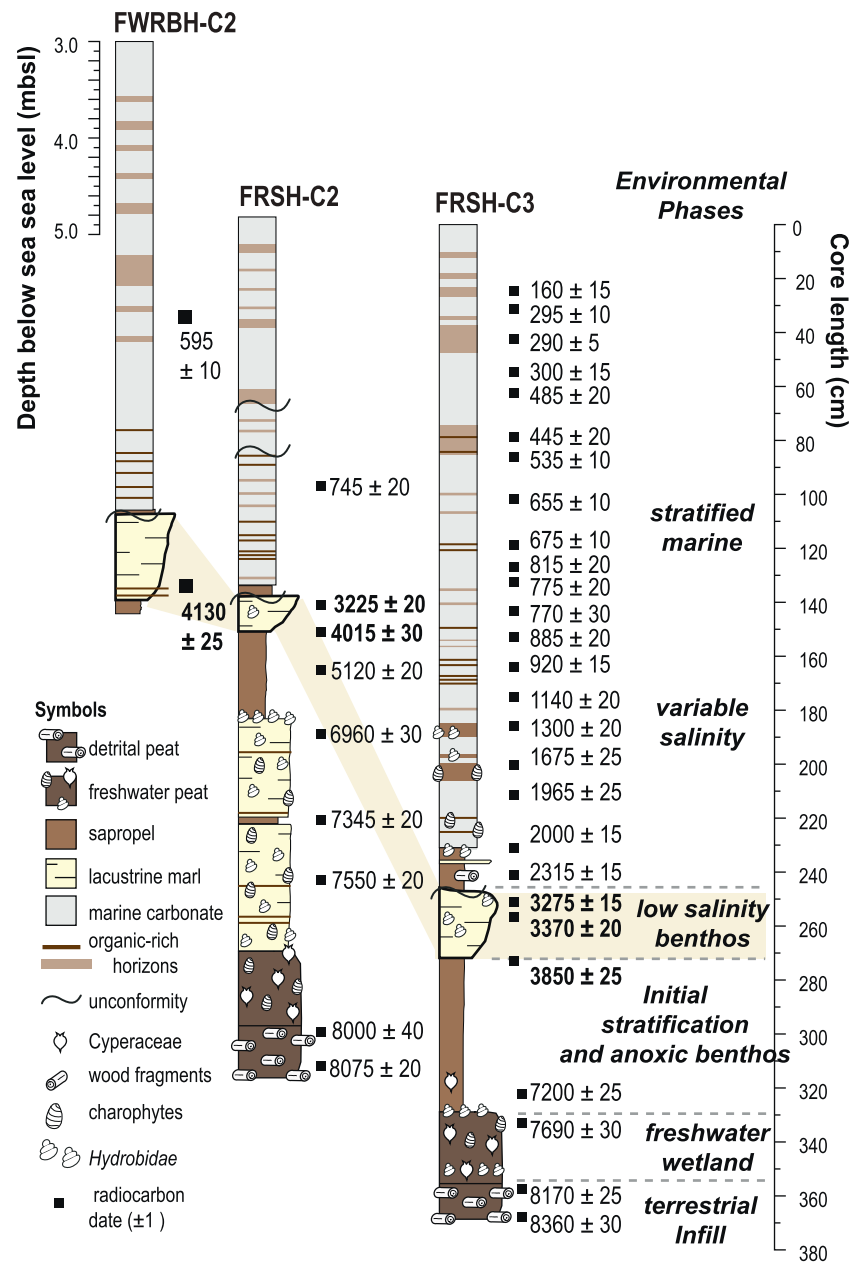
Fig. 3. Stratigraphic columns, radiocarbon dates, and long-term environmental phases. Note that the left vertical axis is the depth of the sediment water interface where the core was collected (mbsl, see also Fig. 2), and the right vertical axis is the sediment core length (cm). Note: mbsl is meters below sea level.

van Hengstum et al., 2018). *Darwinula stevensoni* is particularly significant since it prefers salinities < 2 psu (Keyser, 1977; Holmes, 1997; Pérez et al., 2010). The fragmental granular peat also contained many achenes attributable to the Cyperaceae (c.f. *Torulinium* sp. Koyama, 1976), as well as gyrogonites of charophytes (Fig. 6). Charophytes are macroscopic green algae that colonize fresh to oligohaline waters, and preservation of their calcified fructifications (gyrogonites) in the sediment record is often an indicator of limnic to slightly brackish water (Soulié-Märsche, 2008; Soulié-Märsche and García, 2015; Sand-Jensen et al., 2019).

4.2. Shallow-water lacustrine deposition: ~7600 to 7000 cal yrs BP

Palustrine-lacustrine marl deposition began in FRSH-C2 by 7550 ± 20 cal yrs BP and persisted until 6960 ± 30 cal yrs BP (183–270 cm). The palustrine-lacustrine marl unit in FRSH-C2 had a mean of 13 ± 5% of organic matter (range: 8 to 32%, *n* = 79, Fig. 4),

and had interspersed beds of increased organic matter. No evidence of desiccation (e.g., carbonate hardpan, cracking) was observed to suggest complete drying-out of the lacustrine marl unit during deposition. An increase in localized macrophyte abundance may have generated these organic-rich beds as described by (Alonso-Zarza and Wright, 2010), but vertical root traces were not observed. The ostracodes *Cypridopsis vidua* and *Limnocythere floridensis* were also present (Fig. 6), which colonize low salinity (oligohaline: 0.5 to 3.5 psu) to freshwater aquatic settings (Teeter, 1980). Lacustrine marl did not accumulate at the site of FRSH-C3, which instead documents an abrupt transition to sapropel by 7200 ± 25 cal yrs BP (330 cm in FRSH-C3). At the base of the sapropel in FRSH-C3 are achenes of Cyperaceae, which are the macrofossil remains of a sedge.

4.3. Sapropel deposition ~7200 to 4100 cal yrs BP

By 7200 ± 25 cal yrs BP in FRSH-C3 (~330 cm) and by
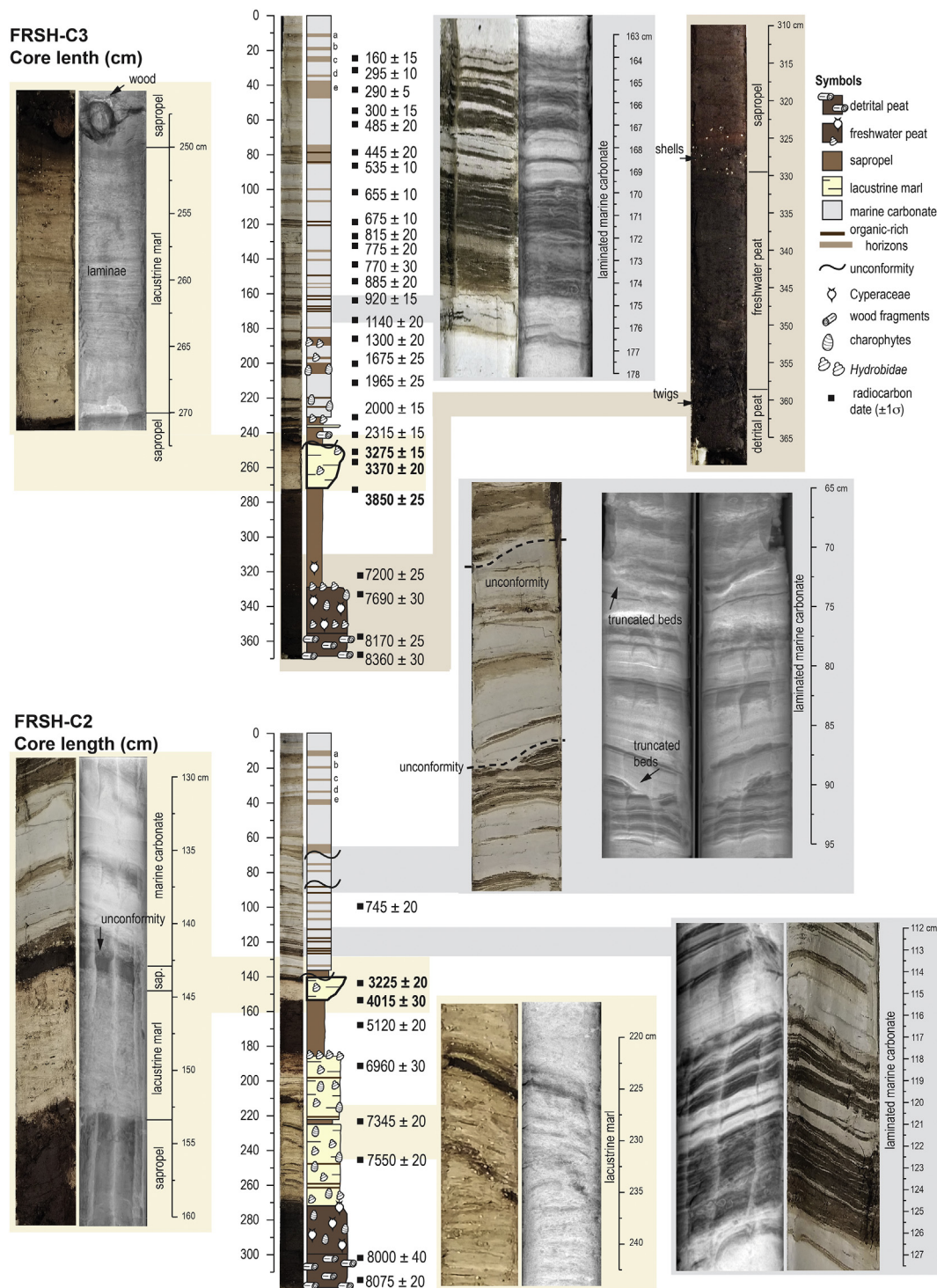
Fig. 4. Detailed photographs and x-radiographs of primary sedimentary facies. See Fig. 3 for symbols.

6960 ± 30 cal yrs BP in FRSH-C2 (~182 cm) deposition shifted to algal sapropel throughout Freshwater River Blue Hole. The sapropel unit had a mean 57 ± 20% bulk organic matter (range: 12 to 81%, $n = 100$), and little coarse-grained mineral sediment (mean: 4.3 ± 9.5 mg/cm^3, range: 0.1 to 44.4 mg/cm^3, $n = 100$). Larger organic fragments from the surrounding terrestrial landscape (sticks and leaves) are absent. The sapropel was devoid of benthic meiofauna, which most likely indicates benthic anoxia. In FRSH-C3, the sapropel sedimentation rate was ~0.1 mm/yr.

4.4. Resumed deposition of lacustrine marl from 4100 to 3300 cal yrs BP

Lacustrine marl sedimentation resumed at 4130 cal yrs BP in FWRBH-C2, and resumed throughout Freshwater River Blue Hole by 3850 ± 25 cal yrs BP. This produced an additional 7 to 20 cm thick carbonate deposit, and sedimentation rate of this unit was ~0.4 mm/yr in FRSH-C3 (Fig. 7). The oligohaline ostracode *Limnocythere floridensis* was preserved throughout the unit, indicating oxygenated and low salinity benthic conditions. The sediments are remarkably similar to the older lacustrine marl in core FRSH-C2, with a mean bulk organic matter
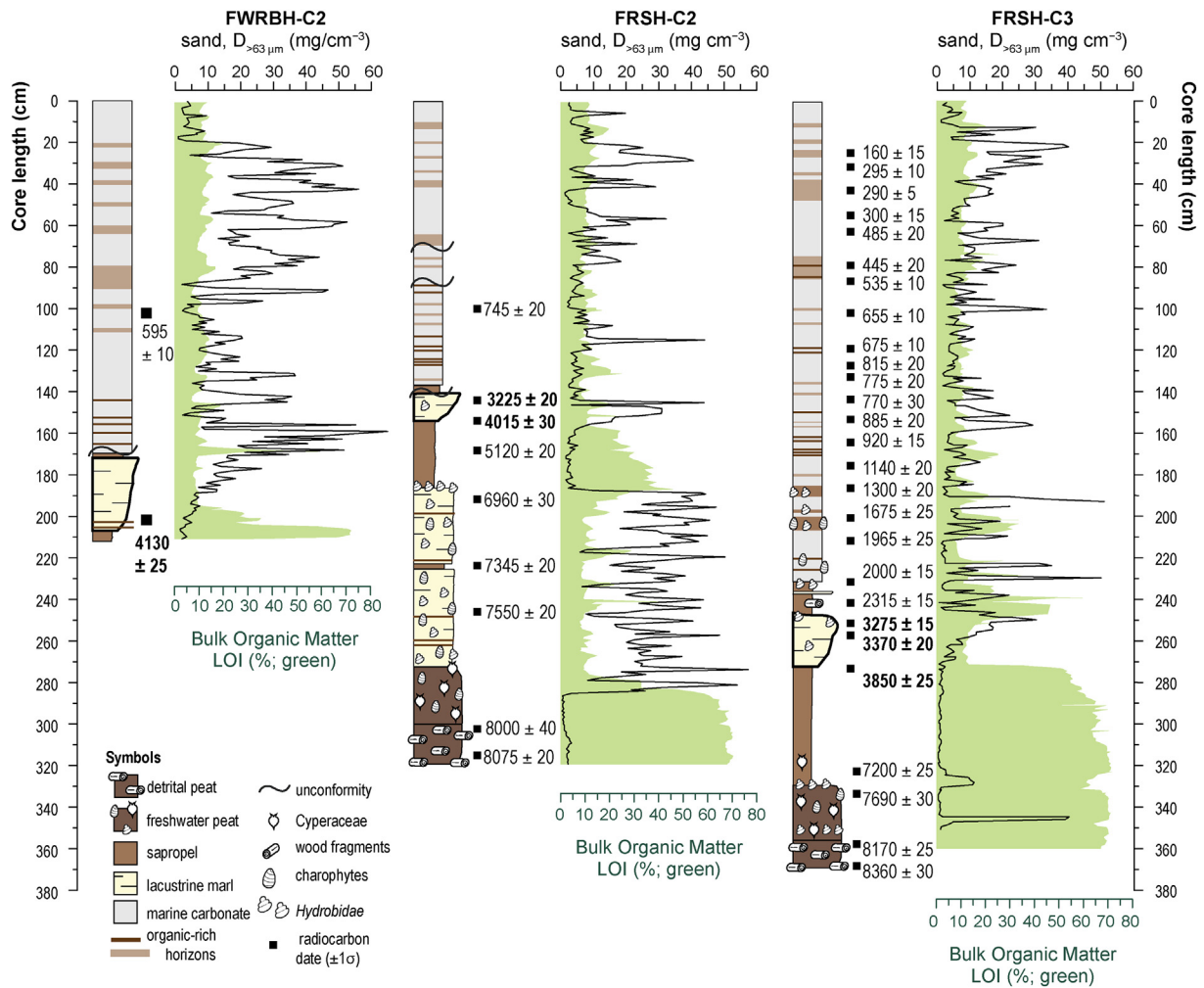
Fig. 5. Downcore coarse-grained particle deposition (Sieve-first LOI, D > 63 μm) and bulk organic matter (Classic LOI, weight %).

of 14 ± 7% (range: 8 to 38%, $n = 77$) and 8.5 ± 2.1 mg/cm^3 (range: 2.1 to 44.0 mg/cm^3, $n = 77$) of coarse-grained mineral material. No evidence of drying-out was observed at the top of this unit (e.g., cracks, hardpans). In all cores, a period of negligible sedimentation (i.e., hiatus) occurs from ~3300 to 2300 cal yrs BP.

4.5. Bedded carbonate mud: 2300 cal yrs BP to present

Deposition shifted at ~2300 cal yrs BP to fine grained carbonate sediment (primarily silt-sized particles) that is repetitively interrupted by organic-rich beds (up to 5 cm thick) and laminations (< 1 cm thick). If the entire unit is averaged, the overall mean bulk organic matter content is 13 ± 6%, but the organic content overall exhibits a considerable range of 7 to 65% ($n = 545$). In FRSH-C3, the bedded carbonate mud experienced two different sedimentation rates: (a) 0.5 to 1.0 mm/yr from ~2300 cal yrs BP to 1050 ± 50 cal yrs BP, and (b) 2 mm/yr from 1050 ± 50 cal yrs BP to present (Fig. 7). The lower and older part of the bedded carbonate mud unit (FRSH-C3, 160 to 240 cm) was only present in FRSH-C3, indicating a depositional hiatus in FRSH-C2 and FWRBH-C2. In FRSH-C3 from ~2300 to 1050 cal yrs BP, the organic-rich intervals were often thicker and occasionally contained gyrogonites from charophytes. For example, there are organic-rich layers with charophytes from 189 to 194 cm (~1315 to 1423 cal yrs BP) and 204–211 cm (~1648 to 1746 cal yrs BP). These organic-rich layers with increased charophytes suggest that at least some part of the water column freshened during their deposition.

In the younger section of the bedded carbonate mud

(1050 cal yrs BP to present), the organic-rich beds and laminations can be correlated between core sites. For example, a distinctive sequence of laminations can be correlated between FRSH-C3 from 164 to 177 cm to FRSH-C2 from 112 to 127 cm (Fig. 4). Based on the age model from FRSH-C3, this salient set of laminations was deposited in ~170 years, from ~936 cal yrs BP (164 cm, 2σ range: 894–1008 cal yrs BP) to ~1107 cal yrs BP (177 cm, 2σ range: 1049 to 1188 cal yrs BP). The preservation of laminations that can be correlated throughout the cores implies negligible bioturbation or vertical sediment mixing. In FRSH-C2, however, two erosive contacts with truncated laminations were observed (~72 cm, ~90 cm). No erosive contacts or truncated beds were observed in FRSH-C3.

Overall, the coarse sedimentary particles (sand-sized and greater) observed were not primarily sourced from the adjacent carbonate tidal flat. The mean coarse-grained mineral content of the unit was $D_{63\,um}$ 13.1 ± 12.1 mg/cm^3 (range: 0.4 to 65 mg/cm^3, $n = 547$) with many intervals having no sand-sized particles at all. Further microscopic examination of the coarse sediment fraction (particle sizes > 63 μm) indicates a primarily in situ (autochthonous) source of the coarse sediment particles. The benthic foraminifer *Peneroplis* was never observed in the stratigraphy from Freshwater River Blue Hole, yet this individual is abundant on the carbonate tidal flats of The Bahamas (discussed further below). For example, one of the coarsest layers observed (19–20 cm depth) contains no *Peneropolis*, only monospecific broken shells of an unidentified bivalve likely derived from inside the blue hole, and a notable dominance of the benthic foraminifer *Ammonia beccarii*. The broken and in situ source of bivalve shells suggests that
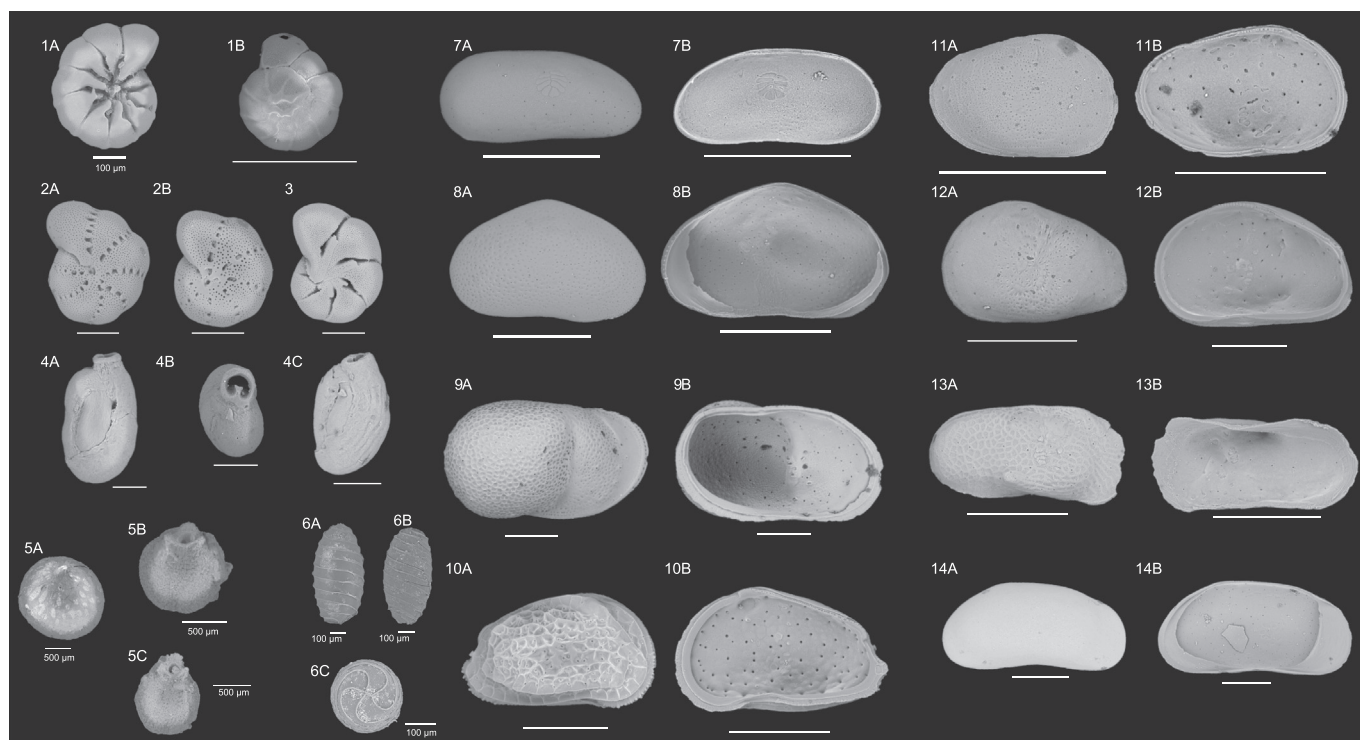
Fig. 6. Scanning electron micrographs of representative microfossils. (**1A**, **B**) *Ammonia beccarii* (Linnaeus, 1758; **a**: ventral, **b**: dorsal); (**2A**, **B**) *Elphidium poeyanum* de Montfort, 1808 (a, b: side view); (**3**) ventral view of *Helenina anderseni* (Warren, 1957); (**4A–C**) *Triloculina* spp. (**a**, **b**: side view, **c**: aperture with tooth); (**5A–C**) achenes from a Cyperaceae; a: bottom view, b, c: apertural view; (**6A–C**) charophyte gyrognites; a, b: side view, **c**: bottom view; (**7A**, **B**) *Darwinula stevensoni* (Brady and Robertson, 1870); (**8A**, **B**) *Cypridopsis vidua* (Müller, 1776); (**9A**, **B**) *Cytheridella ilosvayi* Daday, 1905; (**10A**, **B**) *Malzella floridana* (Benson and Coleman, 1963); (**11A**, **B**) *Loxoconcha matagordensis* Swain, 1955; (**12A**, **B**) *Cyprideis americana* (Sharpe, 1908); (**13A**, **B**) *Limnocythere floridensis* Keyser, 1975; (**14A**, **B**) *Candona annae* (Mehes, 1914). Scale bars represent 250 μm, unless it is otherwise specified.

hurricanes might be impacting sedimentation within the blue hole itself, which is comparable to what has been observed in a larger diameter sinkhole on the Yucatan Peninsula (Brown et al., 2014). Lower in the unit (deeper than 80 cm in FRSH-C3), the coarse layers were nearly 100% *Ammonia beccarii* tests and coincided with the organic-rich layers. *Ammonia beccarii* is a cosmopolitan foraminifera that is tolerant of brackish and dysoxic conditions, and is an early colonizer of newly-available organic-rich benthic habitats. In contrast, the coarse layer from 66 to 67 cm contains an increase in juvenile miliolid benthic foraminifera from the genera *Quinqueloculina* and *Triloculina*, but neither *Ammonia beccarii* nor *Peneroplis*. These microfossil observations indicate that the sedimentary process acting to generate the coarse beds in Freshwater River Blue Hole have been inconsistent over the last 2300 years, and cannot be confidently ascribed to only hurricane overwash.

5. Discussion

5.1. Blue hole environmental and sedimentary history

Basal sediment in Freshwater River Blue Hole is a 10 cm thick fragmental herbaceous peat (plant fragments: > 2 mm, detrital peat in Figs. 3, 4, and 5) that was depoisted from ~8300 to 8100 years ago. The push core FWRBH-C2 did not penetrate deep enough into the sub-surface to sample these older deposits. The lack of environmentally diagnostic microfossils or rootlets (see Kovacs et al., 2013; Gabriel et al., 2009) suggests that this layer was generated by organic matter eroding into the blue hole from the adjacent terrestrial landscape (*Phase 1*, Fig. 9).

The timing for the inundation of Freshwater River Blue Hole by groundwater is consistent with evidence for environmental change on the Little Bahama Bank carbonate platform top caused by the linkage of Holocene sea-level rise to the local groundwater system (Fig. 8). As previously introduced, the deepest area (10.87 mbsl) in the Bight of Abaco transitioned from a terrestrial landscape to a freshwater aquatic environment ~8790 years ago (Rasmussen et al., 1990). The Bight of Abaco was originally flooded from within on the dish-shaped Pleistocene topography by an upward migrating freshwater (meteoric) lens from Holocene sea-level rise (Rasmussen et al., 1990).

The bottom of Freshwater River Blue Hole at 8.9 ± 0.2 mbsl flooded at 8170 ± 25 cal yrs BP (Table 1), which is consistent with a vertically rising meteoric lens in the subsurface from Holocene sea-level rise. A fragmental granular peat (plant fragments: 0.1 to 2 mm, freshwater peat in Figs. 3, 4, and 5) was deposited from ~8100 to 7600 years ago, which is consistent with emplacement of a freshwater wetland (*Phase 2*, Fig. 9). The preserved microfossils (ostracodes and charophyte remains) indicate that the salinity of the meteoric lens that first flooded Freshwater River Blue Hole was likely in the low brackish range (freshwater to oligohaline: 0 to ~3.5 psu). Inundation of Freshwater River Blue Hole is younger than the bottom of the Bight of Abaco, but this is expected given the base of the blue hole is shallower than the deepest area in the Bight of Abaco (Fig. 8). It is important to note that Freshwater River Blue Hole would have been located on the terrestrial landscaped surrounded by a subtropical forest ecosystem during the middle Holocene, and not surrounded by carbonate tidal flats.

The freshwater peat deposits in Freshwater River Blue Hole are a maximum sea-level indicator for the area (terrestrial limiting), which can be used to constrain local glacio-isostatic processes (Hibbert et al., 2018). Indeed, the age and depth of the freshwater peat deposits compare closely with modelled estimates of relative sea-level rise for The Bahamas (Fig. 8). The Freshwater River Blue Hole peat deposits developed in similar environmental conditions as the freshwater peat deposits in Mullet Pond in northwestern Florida, USA (Lane et al., 2011), and Mangrove Lake in Bermuda (Hatcher et al., 1982; Watts and
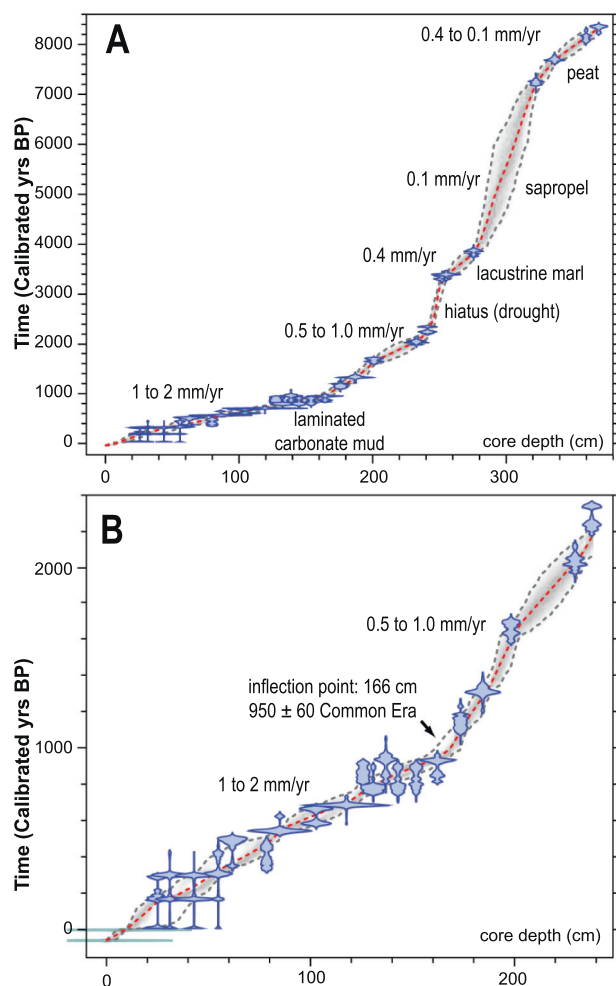
Fig. 7. The Bayesian age models and sedimentation rates for FRSH-C3 for the (A) entire sediment record, and (B) only the upper bedded carbonate mud unit.

Hansen, 1986). One would expect that a vertically migrating coastal aquifer would cause a blue hole to first become flooded by a meteoric lens , which is the upper fresh to brackish groundwater mass of carbonate aquifers. For different study sites, however, one must still consider that multiple factors can impact the salinity, thickness, and development of meteoric lenses on carbonate platforms, such as: inherited lithology, subsurface elevation of confining layers or porosity, hydraulic conductivity (Budd and Vacher, 1991; Whitaker and Smart, 1997; Ritzi Jr. et al., 2001), carbonate platform/island size (Cant and Weech, 1986; Whitaker and Smart, 1997), regional rainfall and evaporation (water balance), proximity to the ocean (Martin et al., 2012; Kovacs et al., 2017), and the proximity of a blue hole to a carbonate platform margin where groundwater de-stratification and mixing occurs from tidal and wave action.

From ~7600 to 7000 cal yrs BP, the shallower sites (FRSH-C2) in Freshwater River Blue Hole were accumulating lacustrine marl at the same time as the slightly deeper site (FRSH-C3) was accumulating sapropel (*Phase 3*, Fig. 9). Interestingly, the lower part of the sapropel did contain some Cyperaceae achenes (~322 cm in FRSH-C3, Fig. 5), however, this is expected given these plants were living < 10 m away at the shallower locality (FRSH-C2). Based on the radiocarbon ages, it is likely that lacustrine marl was accumulating in the shallow locations (FRSH-C2), and laterally intergraded into sapropel in the deeper location in the deeper locality (FRSH-C3). Lacustrine marl is commonly deposited in groundwater-fed aquatic basins when groundwater is supersaturated with respect to carbonate (Street-Perrott et al., 1993; Holmes, 1998; Alonso-Zarza and Wright, 2010). Similar lacustrine marl

accumulated during the middle Holocene in the nearby No Man's Land sinkhole-lake soon after it became a shallow limnic environment (van Hengstum et al., 2018). In nearby Cuba, lacustrine marl that accumulated during the middle Holocene in Cenote Jennifer was likely caused by similar environmental conditions (Peros et al., 2017). Based on the recovered sediment cores, the difference between the lacustrine marl in FRSH-C2 and the sapropel deposits in FRSH-C3 was < 1 m depth, with a spatial range of < 10 m (Figs. 2, 3). These results indicate the sensitivity of autogenic sedimentation in blue holes to variations of accommodation space of < 1 m caused by the inherited limestone floor or collapse breccia.

Rising water levels eventually allowed a stratified water column to develop within Freshwater River Blue Hole from ~7000 to 4100 years ago (*Phase 4*, Fig. 9). The lack of any benthic meiofauna throughout this interval indicates a continuous lack of oxygen at the sediment-water interface. This is consistent with the benthos becoming flooded by low oxygen marine or brackish water from local groundwater-level rise. A change to sapropel deposition alone cannot be used to infer regional rainfall changes, since sapropel is currently accumulating in shallow sinkholes in Long Island in The Bahamas (~900 mm/yr rainfall: Jury et al., 2007) and Mangrove Lake in Bermuda (~1450 mm/yr rainfall: Hatcher et al., 1982). Indeed, a shift from lacustrine marl to sapropel deposition in No Man's Land in Abaco Island was interpreted as related to the onset of more arid conditions from ~3300 to 2500 cal yrs BP (van Hengstum et al., 2018), but this was in conjunction with benthic microfossil data that indicated an abrupt change in water column stratification and benthic conditions during a period with negligible vertical change in groundwater level. In comparison to the middle Holocene stratigraphy in Freshwater River Blue Hole, the rates of groundwater-level rise would have been higher during the middle Holocene (Fig. 5), which would have eventually flooded the benthos by a low-oxygen saline water mass as part of the local coastal aquifer. These comparisons indicate that sapropel deposition in a blue hole is not necessarily diagnostic of regional paleoenvironmental change, but must be first evaluated relative to vertical changes in the local coastal aquifer.

Interestingly, there is no evidence of environmental change in Freshwater River Blue Hole caused by the transition of the Bight of Abaco into a marine lagoon. In terms of surface hydrology, the Bight of Abaco abruptly shifted from an inland fresh-to-brackish lake to a marine carbonate lagoon at 5900 to 5500 years ago (Rasmussen et al., 1990). This occured when Holocene sea-level rise flooded the sill between Moore's Island (see Fig. 2) and Grand Bahama Island (Rasmussen et al., 1990). This change rejuvenated accretion of the offshore Holocene wedge on the northern Little Bahama Bank as a consequence of increased export of carbonate sediment from the bank top (Fauquembergue et al., 2018). From a hydrogeological perspective, a broad meteoric lens in the subsurface would have changed, potentially dividing in half, with remaining portions back-stepping towards the islands of Grand Bahama and Great Abaco (Gulley et al., 2016). Perhaps Freshwater River Blue Hole was still far enough inland and away from the Bight of Abaco paleo shoreline to be insensitive to the regional groundwater changes caused by this event.

From ~4100 to ~3200 years ago (*Phase 5*, Fig. 9), there was an abrupt reversion to lacustrine marl deposition (Figs. 9, 3) and colonization of the benthic ostracode *Limnocythere floridensis*. This ostracode is well known from tropical and subtropical low salinity aquatic habitats in the North Atlantic region (Keyser, 1977; Teeter, 1980). This indicates a breakdown in water column stratification, increased benthic dissolved oxygen levels, and reversion of the benthos back to low salinity (oligohaline) or freshwater conditions at ~4100 years ago. A drop in sea-level would potentially expose the sediment-water interface to more oxygenated water of a local meteoric lens, if the coastal aquifer vertically dropped. However, regional sea-level reconstructions provide no evidence for a sea-level drop between ~4100 and 3200 years ago (Milne and Peros, 2013; Khan et al., 2017). Island area is regarded as one of the most important predictors of meteoric lens volume (i.e.,
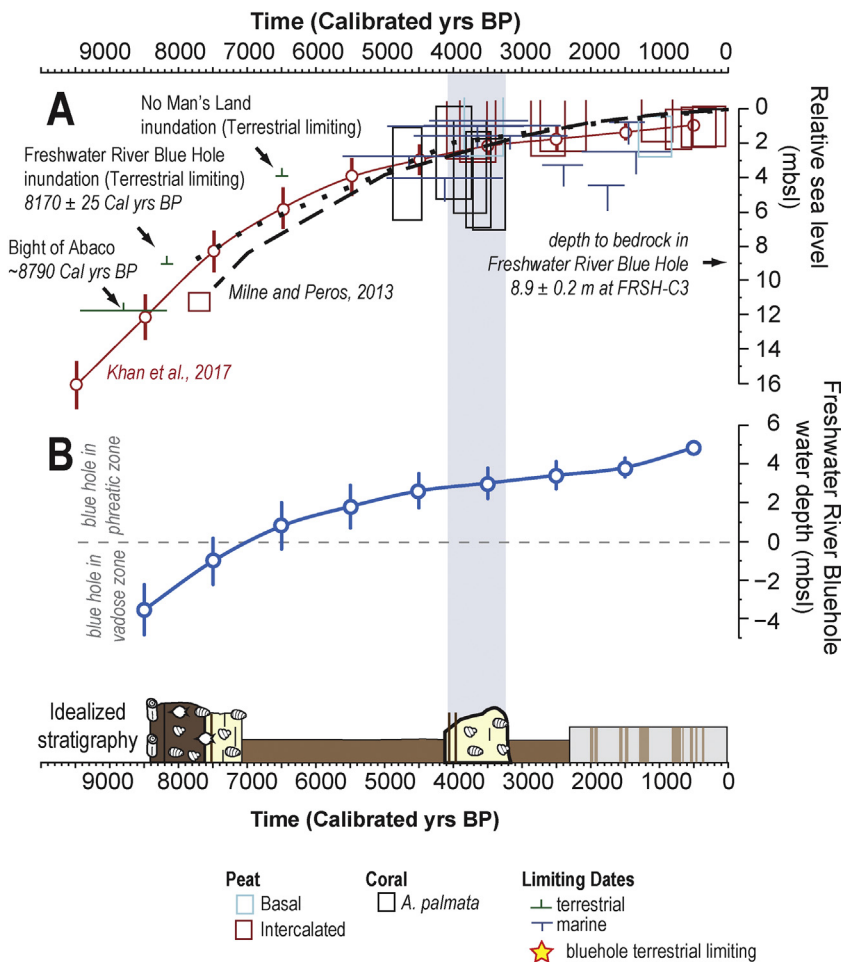
Fig. 8. (A) Evidence for Holocene relative sea-level rise in the northern Bahamas versus groundwater inundation and fill of the Freshwater River Blue Hole. Regional sea-level indicators and resultant sea-level curve-after Khan et al. (2017), with additional older sea-level indicators from Abaco Island (Neumann and Land, 1975; Rasmussen et al., 1990; van Hengstum et al., 2018). ICE-5G model results with an upper mantle viscosity (UMV) = 5×10^{21} Pas and lower mantle viscosity (LMV) of 5×10^{22} Pas (dotted line) and EUST3 with an UMV = 2×10^{21} Pas and LMV = 5×10^{22} Pas (dashed line) (Milne and Peros, 2013). These results indicate that a freshwater marsh developed in Freshwater River Blue Hole at 8170 ± 25 cal yrs BP [2σ calibration and probability: 8023–8213, 0.938] at 8.4 ± 0.2 m below modern sea level is within uncertainty estimates for the coeval position of relative sea level in the northern Bahamas. (B) Estimate of water column deepening in the Freshwater River Blue Hole through the Holocene, under the assumption that water table deepening in the blue hole closely followed Holocene relative sea-level rise through the porous antecedent lithology [e.g., estimated hydraulic conductivity of 86.4 m/day: (Holding and Allen, 2015)]. Blue shaded window highlights timing of potential pluvial event in Abaco Island from 4100 to 3300 years ago. (For interpretation of the references to color in this figure legend, the reader is referred to the web version of this article.)

larger island area = larger meteoric lens; Cant and Weech, 1986; Whitaker and Smart, 1997). However, continuous sea-level rise should reduce island area and meteoric lens volume, and in turn reduce the potential for fresh groundwater to have flooded Freshwater River Blue Hole from 4100 to 3200 years ago. Observations in North Andros, which has similar hydrogeology and hydroclimate to Abaco Island, indicate that the alternation between wet and dry seasons may result in up to 1 m vertical expansion and contraction of the freshwater lens, respectively (Whitaker and Smart, 1997). If these seasonal processes were amplified by a centennial-scale megadrought, perhaps a more negative regional water balance (e.g., decreased rainfall or increased evaporation) would amplify freshwater loss, upward vertical contraction of the meteoric lens and halocline, and promote flooding of the benthos by saline groundwater. In contrast, the sedimentary observations combined with these hydrogeologic principles suggest the *opposite* occurred in Freshwater River Blue Hole: the benthos became flooded by low salinity water, and this would potentially indicate a more *positive* regional water balance and increased aquifer recharge from ~4100 to ~3300 years ago. The potential for a wetter climate on Abaco from 4100 to 3200 years warrents further investigation.

At ~3200 years ago, deposition in Freshwater River Blue Hole became negligible (*Phase 6*, Fig. 9) based on the radiocarbon results between 240 and 250 cm in FRSH-C3. As such, there is likley an unconformity in FRSH-C2 (~137 cm) and FWRBH-C2 (~117 cm) between the lacustrine marl and bedded carbonate mud (Fig. 3). Previous results indicate that Abaco experienced a drought from ~3200 to 2500 cal yrs BP. This is based upon the abrupt salinization and stratification of a sinkhole-lake (van Hengstum et al., 2018), and the expansion of grasses in central Abaco (Slayton, 2010). There is evidence

for arid conditions elsewhere in the Caribbean during this period, including Cuba and Hispañiola (see discussion in van Hengstum et al., 2018). Despite regional aridity, there is no evidence that Freshwater River Blue Hole dried out (e.g., hardpans), therefore the site must have remained hydrographically connected to the regional aquifer system.

Based on the radiocarbon dates in FRSH-C3, a bedded carbonate mud unit began deposition ~2300 years ago (*Phase 7*, Fig. 9). Given the slightly lower position of sea level ~2300 years ago relative to present (~1.5 m, Fig. 8), the onset of carbonate mud deposition is likely not caused by sea-level overtopping the periphery of Freshwater River Blue Hole, which is only < 0.5 m deep at modern high tides. This subtle feature has not been previously illustrated in previous conceptual models of blue hole environmental change in response to sea-level rise (Shinn et al., 1996; van Hengstum et al., 2011; Gregory et al., 2017). In comparison to further illustrate the point, a blue hole on nearby Grand Bahamas Island (Fig. 1B, Dead Pines: 26.669 N, −78.235 W) that is positioned ~800 m inland from the shoreline is already accumulating marine carbonate mud in an oxygenated marine setting (van Hengstum, Sullivan, Winkler, pers. obs.). It is perhaps unsurprising that carbonate mud deposition in Freshwater River Blue Hole predates inundation of the blue hole periphery by sea-level rise. This is because the aquatic conditions in groundwater-fed blue holes is linked to local coastal aquifer hydrodynamics, and groundwater proximal to the shoreline is impacted by tidal and wave mixing, de-stratification, and regional characteristics like subsurface lithology (Whitaker and Smart, 1997; Martin et al., 2010). As a result, the groundwater proximal to the shoreline on carbonate landscapes is often brackish or marine (Whitaker and Smart, 1997). Taken collectively, it is likely that the aquatic conditions within a blue hole will become marine prior to

Phase 1. 8300 to 8100 years ago

Phase 2. 8100 to 7600 years ago

Phase 3. 7600 to 7000 years ago

Phase 4. 7000 to 4100 years ago

Phase 5. 4100 to 3300 years ago

Phase 6. 3300 to 2300 years ago

Phase 7. 2300 years ago to present
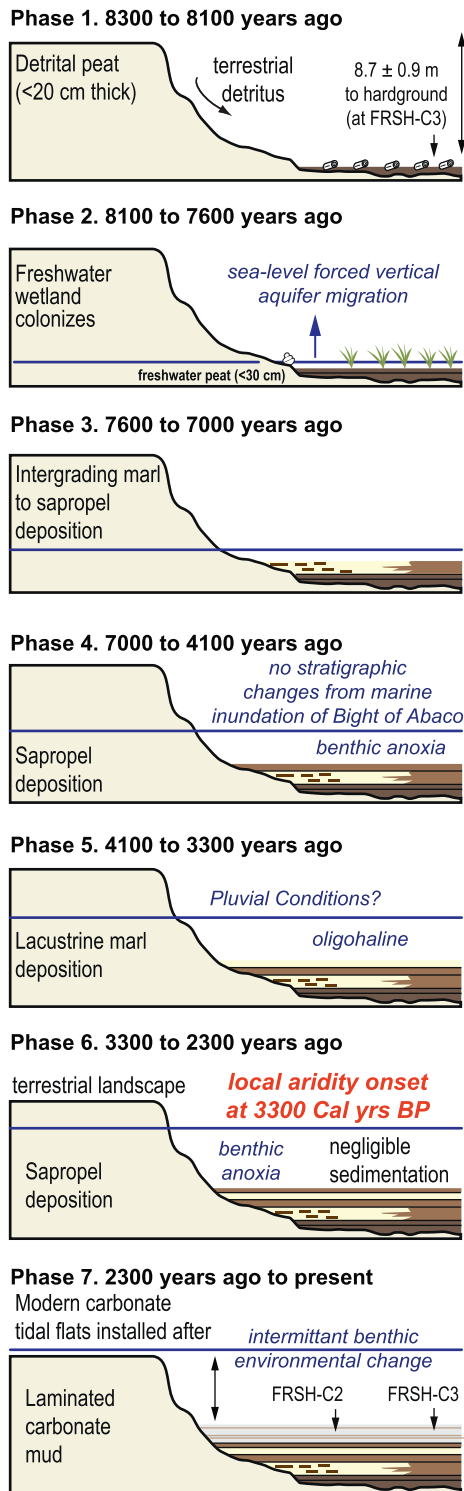
Fig. 9. A conceptual model that illustrates environmental change in Freshwater River Blue Hole over the last ~8300 years. (For interpretation of the references to color in this figure legend, the reader is referred to the web version of this article.)

simple geometric inundation of the periphery by sea-level rise. The stratigraphy archived in Freshwater River Blue Hole clearly documents this process.

During the earlier period of bedded carbonate mud deposition from ~2300 to 1050 cal yrs BP with lower sedimentation rates (0.5–1.0 mm/yr), some of the organic-rich intervals contained charophyte remains (Fig. 3). These observations imply the benthos was intermittently

flooded with fresh to slightly brackish groundwater. It is possible that the earlier period of bedded carbonate mud is documenting the onset of marine-dominated conditions in the blue hole, with oscillating salinity at the benthos. Alternatively, the organic-rich horizons may reflect changing groundwater stratification in the blue hole related to regional aquifer recharge. Detailed paleoecological analysis of microfossils (ostracodes and foraminifera) is required to ascertain the nature, significance, and timing of organic matter beds and laminations, and their potential linkage to hydrographic changes during the last 2300 years.

5.2. Hurricane impacts

Offshore and subtidal blue holes like the Great Belize Blue Hole on Light House Reef (Gischler et al., 2008; Denomee et al., 2014), and nearby Thatchpoint Blue Hole on Abaco (van Hengstum et al., 2014), contain sedimentary evidence of hurricane passage. Given the location of Freshwater River Blue Hole within the carbonate tidal flats of The Marls and the relatively high incidence of hurricanes striking Abaco, the preservation of hurricane-induced event beds would be expected. As van Hengstum et al. (2014) observed, hurricane tempestites in blue holes are not necessarily distinctive sand layers. For example, hurricane passage can be represented by an increase of coarse particles within a fine-grained sedimentary matrix, which is ultimately linked to storm characteristics (e.g., translational velocity, tidal phase at landfall, offshore vs. onshore wind patterns) and regional factors (e.g., local sediment budgets, and topography). Freshwater River Blue Hole shows an overall coarsening upwards trend in the coarse sediment fraction, with frequent oscillations between lower ($D_{>63\mu m} < 7\,\text{mg cm}^{-3}$) and higher ($D_{>63\mu m} > 13\,\text{mg cm}^{-3}$) coarse sediment content (Fig. 4).

One of the most intense hurricane strikes on Abaco within the instrumental record (since 1851 CE) occurred in 1932 CE with sustained 1-minute winds of 72 m/s (category 5 on the Saffir-Simpson Scale), and the circulation center of this storm passed ~14 km west of Freshwater River Blue Hole. Of course, the sediment cores were collected prior to Hurricane Dorian in 2019, so the impact of this intense storm on the study site is unknown. Based on our age model, however, the topmost coarse deposit in FRSH-C3 at 12–13 cm depth was deposited ~1932 CE (2σ age range: 1895 to 1955 CE), and it is likely that the unnamed 1932 CE storm and coarse horizon are related. However, more recent less intense landfalls in Abaco like Irene (2011, cat. 2) and Floyd (1999, cat. 3) cannot be associated to a significant coarse bed in FRSH-C3. While the circulation center of these storms passed very close to Freshwater River Blue Hole, the wind direction at maximum intensity were easterly and thus blowing offshore, which likely minimized the potential for storm surge and subaqueous sediment transport. A large peak in coarse fraction between 21 and 22 cm in FRSH-C3 dates to 1832 CE (2σ age range: 1774 to 1994 CE) and may be related to the 1866 CE category 4 hurricane that passed 60 km west of Freshwater River Blue Hole. The trajectory of the 1866 hurricane would have caused the strongest winds from the southwest at the study site. Winds from this quadrant should have piled surge and waves in The Marls, and heightened the potential for hurricane deposition in Freshwater River Blue Hole. Upon microscopic examination, however, the coarse intervals in Freshwater River Blue Hole, including the layers at 12–13 cm and 20–23 cm, do not contain microfaunal remains derived from the adjacent carbonate tidal flats.

The ecological range of many benthic foraminifera are zoned with respect to benthic habitats in the coastal and subtidal zones, and their subfossil shells are well known sediment provenance and transport proxies (Lane et al., 2011; Pilarczyk et al., 2014). On the leeward western side of both Abaco Island (Bight of Abaco) and Andros Island (western Great Bahama Bank), the large benthic foraminifera *Peneroplis proteus* (> 1 mm in diameter) is very common in the subtidal and intertidal zones (Todd and Low, 1971; Rose and Lidz, 1977). Relative to subtidal zones, the proportion of *Peneroplis* increases in quiescent tidal flats of Andros Island, Crooked Island, and Caicos Island (Berkeley and

Rankey, 2012; Maloof and Grotzinger, 2012). Surprisingly, *Peneroplis* tests were not observed – in any – coarse horizons preserved the Freshwater River Blue Hole (see results above), including coarse deposits in FRSH-C3 at 12–13 cm and 21–22 cm. Instead, the deposit is dominated by the foraminifera *Ammonia beccarii*, which is an indiscriminating and cosmopolitan species known from brackish to marine environments, and from oxygenated to dysoxic settings. While other coarse horizons also lacked *Peneroplis*, they in contrast contained an increase in other miliolid taxa and not *Ammonia* (e.g., *Quinqueloculina*, FRSH-C3 from 66–67 cm). In addition, both of these examples also contained negligible Cerithid gastropods (e.g., *Batillaria*), which are also abundant on the Bahamian carbonate tidal flats. Our microfossil-based sedimentary provenance analysis (e.g., lack of *Peneroplis*) provides conclusive evidence that classic hurricane overwash processes are not the primary driver of coarse particle deposition at FRSH-C3 (i.e., from the carbonate tidal flats into the blue hole).

Given the abundant regional sediment supply and energy associated with hurricane events it is difficult to explain the lack of overwash deposits in Freshwater River Blue Hole. However, we are not the first to observe that hurricane events can occasionally cause minimal impact to carbonate tidal flats. Hurricane Michelle (category 1) on 5 November 2001 caused very little sedimentological impact to western Andros Island (Rankey et al., 2004). Similarly, passage of Hurricane Betsy (1965) flooded the northern tidal flats of Andros with 3 m of water (demonstrated by debris in trees), but resulted in negligible sediment deposition on the tidal flats (Perkins and Enos, 1968). After landfall of Hurricane Kate in 1985 on the Caicos Platform as a category 1–2 event (Saffir-Simpson Scale), Wanless et al. (1987) noted that although no expansive subtidal tempestite was deposited on the platform interior, coarse-grained particles were trapped in Callianassid shrimp burrows. Using satellite observations, Reeder and Rankey (2012) specifically noted very little geomorphologic change to the Abaco carbonate tidal flats after historical hurricane events in 2004 CE. These other authors specifically noted how these hurricane events minimally impacted the carbonate tidal flats, and often called for increased instrumentation and physical measurements during hurricane passage to help understand this riddle. It is worth nothing that sedimentation rate in the intertidal Freshwater River Blue Hole has been only 1–2 mm/yr over the last 1000 years, whereas sediment records from other Bahamian blue holes in similar subtidal positions (Caicos Blue Hole: 21.719, −71.812; Long Island Blue Hole: 23.264, −75.117, Cay Sal Bank Blue Hole: 23.864, −79.804) have an order of magnitude higher sedimentation rate of ~1 cm/year.

Recently, Sahoo et al. (2019) modelled storm surge, significant wave height, and coastal currents in the Bahamian archipelago using ADCIRC-SWAN output during passage of Hurricane Joaquin in 2015, which was an intense category 4 event at landfall (Saffir-Simpson Scale). In general, the narrow and steep continental shelves surrounding the carbonate platforms were found to accelerate wave-current activity in the inner shelf region, but coastal morphodynamics can act to buffer the coastlines from greater storm surge impacts. For example, model output indicates that Hurricane Joaquin generated a modest 1.5 m storm surge at the shoreline of multiple Bahamian islands, but effective wave height achieved 3–7 m just offshore (note: variable across the archipelago). Hurricane-induced coastal current speeds also varied between the western and eastern sides of islands, where slower current speeds were observed on the protected western leeward sides of islands. Taken collectively, these results indicate that the ability of any blue hole to be sensitive to hurricane-induced sedimentary overwash will depend upon its proximity to the shoreline, local wave setup and coastal current speeds during hurricane passage in response to coastal geometry, and water depth. It is likely that the peripheral vegetation (i.e., mangroves), the leeward western positioning, and coastal proximity are affording some protection to Freshwater River Blue Hole to classic hurricane overwash sedimentation. These results also potentially explain how blue holes in the vicinity of elevated coastal currents

(proximal to tidal creeks in southern Andros, Wallace et al., 2019) or positioned in slightly deeper water (Thatchpoint Blue Hole in Abaco: van Hengstum et al., 2014; Great Blue Hole in Belize: Gischler et al., 2008) have preserved consistent stratigraphic records of prehistoric hurricane passage.

6. Conclusion

The stratigraphy archived in Freshwater River Blue Hole on Abaco Island in The Bahamas preserves a record of environmental change during the last transgression, and allows for a detailed analysis of autogenic versus allogenic sedimentary processes in blue holes. Holocene groundwater-level and sea-level rise controlled changing environmental conditions in the blue hole, which in turn signficantly impacted the sedimentary facies through time. Sedimentation began ~8300 years ago when a freshwater wetland developed on the blue hole bottom. Changes in water column stratification, involving both salinity and dissolved oxygen, strongly influenced both benthic and pelagic conditions through time. After shallow flooding, freshwater aquatic conditions promoted lacustrine-palustrine marl deposition (~8000 to 7000 years ago), but this passed into sapropel deposition with further groundwater-level rise by 7000 years ago. However, from 7500 to 7000 years ago, intergrading sapropel and lacustrine marl deposits occurred over spatial distances of < 10 m, and were related to subtle bathymetric changes (< 1 m) related to the antecedent limestone. These results indicate that small changes (< 1 m) in accommodation space can promote lateral facies changes in a blue hole during lower water levels. Regional hydrographic and groundwater change caused by marine inundation of the Bight of Abaco (~6000 to 5500 years ago) did not impact paleoenvironmental conditions or blue hole sedimentation. This may be related to Freshwater River Blue Hole being positioned on the terrestrial landscape at this time. In the Late Holocene, a lacustrine marl facies was deposited from 4100 to 3200 cal yrs BP, and this deposit contained benthic microfossils that colonize oxygenated and low salinity habitats. Given the lack of evidence for a sea-level drop at this time, this stratigraphic change might reflect increased aquifer recharge and regional rainfall, but additional groundwater modelling is required to resolve this question. In the last 2300 years, carbonate mud with abundant organic matter beds and laminations were deposited. Despite the abundant local sediment supply, classic hurricane overwash is not the primary driver of sedimentation. Carbonate mud deposition is likely related to the onset of more marine conditions in the blue hole as the shoreline and coastal aquifer migrated proximal to the study site from continued Holocene sea-level rise. The organic-rich laminations present throughout the carbonate mud unit suggest repeated changes in water column stratification, which is perhaps related to regional hydroclimate change during the Common Era.

Data availability

All radiocarbon dates (Appendix 1) are uploaded into an online supplementary dataset associated with this paper.

Appendix A. Supplementary data

Supplementary data associated with this article can be found in the online version, at https://doi.org/10.1016/j.margeo.2019.106051. These data include the Google map of the most important areas described in this article.

References

Adams, A.J., Cooke, S.J., 2016. Advancing the science and management of flats fisheries for bonefish, tarpon, and permit. Environ. Biol. Fish 98, 2123–2131.

Agassiz, A., 1894. A Reconnaissance of the Bahamas and Elevated Reefs of Cuba in the Steam Yacht "Wild Duck", January to April 1893. Bulletin of the Museum of Comparative Zoology at Harvard College 26. pp. 1–203.

Alonso-Zarza, A.M., Wright, V.P., 2010. Palustrine Carbonates. In: Alonso-Zarza, A.M., Tanner, L.H. (Eds.), Carbonates in Continental Settings. Elsevier, Amsterdam, pp. 103–131.

Alverez Zarikian, C.A., Swart, P.K., Gifford, J.A., Blackwelder, P.L., 2005. Holocene paleohydrology of Little Salt Spring, Florida, based on ostracod assemblages and stable isotopes. Palaeogeogr. Palaeoclimatol. Palaeoecol. 225, 134–156.

Ashmore, S., Leatherman, S.P., 1984. Holocene sedimentation in Port Royal Bay, Bermuda. Mar. Geol. 56, 289–298.

Berkeley, A., Rankey, E.C., 2012. Progradational Holocene carbonate tidal flats of Crooked Island, south-east Bahamas: an alternative to the humid channelled belt model. Sedimentology 59, 1902–1925.

Blaauw, M., Christen, A., 2011. Flexible paleoclimate age-depth models using an auto-regressive gamma process. Bayesian Anal. 6, 457–474.

Brandon, C., Woodruff, J.D., Lane, P., Donnelly, J.P., 2013. Constraining flooding conditions for prehistoric hurricanes from resultant deposits preserved in Florida sinkholes. Geochemistry Geophysics Geosystems 14, 2993–3008.

Brown, A., Reinhardt, E.G., van Hengstum, P.J., Pilarczyk, J.E., 2014. A coastal Yucatan sinkhole records intense hurricane events. J. Coast. Res. 30 (2), 418–428. https://doi.org/10.2112/JCOASTRES-D-13-00069.

Budd, D.A., Vacher, H.L., 1991. Predicting the thickness of fresh-water lenses in carbonate paleo-islands. J. Sediment. Petrol. 61, 43–53.

Cant, R.V., Weech, P.S., 1986. A review of the factors affecting the development of Ghyben-Hertzberg lenses in the Bahamas. J. Hydrol. 84, 333–343.

Cole, L.G., 1910. The caverns and people of the northern Yucatan. Bull. Am. Geogr. Soc. 42, 321–336.

Collins, S.V., Reinhardt, E.G., Werner, C.L., Le Maillot, C., Devos, F., Rissolo, D., 2015. Late Holocene mangrove development and onset of sedimentation in the Yax Chen cave system (Ox Bel Ha) Yucatan, Mexico: implications for using cave sediments as a sea-level indicator. Palaeogeogr. Palaeoclimatol. Palaeoecol. 438, 124–134.

Correll, D.S., Correll, H.B., 1982. The Flora of the Bahama Archipelago (Including Turks and Caicos Islands). A.R. Ganter Verglag.

Dean Jr., W.E., 1974. Determination of carbonate and organic matter in calcareous sediments and sedimentary rocks by loss on ignition: comparison with other methods. J. Sediment. Res. 44, 242–248.

Denomee, K.C., Bentley, S.J., Droxler, A.W., 2014. Climatic control on hurricane patterns: a 1200-y near-annual record from Lighthouse Reef, Belize. Sci. Rep. 4, 7.

Droxler, A.W., Schlager, W., Whallon, C., 1983. Quaternary aragonite cycles and oxygen-isotope record in Bahamian carbonate ooze. Geology 11, 235–239.

Fauquembergue, K., Ducassou, E., Mulder, T., Hanquiez, V., Perello, M.-C., Poli, E., Borogomano, J., 2018. Genesis and growth of a carbonate Holocene wedge on the northern Little Bahama Bank. Marine and Petroleum Geology 96, 602–614.

Gabriel, J.J., Reinhardt, E.G., Peros, M.C., Davidson, D.E., van Hengstum, P.J., Beddows, P.A., 2009. Palaeoenvironmental evolution of Cenote Aktun Ha (Carwash) on the Yucatan Peninsula, Mexico and its response to Holocene sea-level rise. J. Paleolimnol. 42, 199–213.

Gischler, E., Shinn, E.A., Oschmann, W., Fiebig, J., Buster, N.A., 2008. A 1500-year Holocene Caribbean climate archive from the Blue Hole, Lighthouse Reef, Belize. J. Coast. Res. 24, 1495–1505.

Gregory, B.R.B., Reinhardt, E.G., Gifford, J.A., 2017. The influence of morphology on sinkhole sedimentation at Little Salt Spring, Florida. J. Coast. Res. 33, 359–371.

Grimm, E.C., Jacobson, G.L., Watts, W.A., Hansen, B.C.S., Maasch, K.A., 1993. A 50,000-year record of climate oscillations from Florida and its temporal correlation with the Heinrich events. Science 261, 198–200.

Gulley, J.D., Mayer, A.S., Martin, J.B., Bedekar, V., 2016. Sea level rise and inundation of island interiors: assessing impacts of lake formation and evaporation on water resources in arid climates. Geophys. Res. Lett. 43, 9712–9719.

Hatcher, P.G., Simoneit, B.R.T., Mckenzie, F.T., Neumann, A.C., Thorstenson, D.C., Gerchakov, S.M., 1982. Organic geochemistry and pore water chemistry of sediments from Mangrove Lake, Bermuda. Org. Geochem. 4, 93–112.

Heiri, O., Lotter, A.F., Lemcke, G., 2001. Loss on ignition as a method for estimating organic and carbonate content in sediments: reproducibility and comparability of results. J. Paleolimnol. 25, 101–110.

van Hengstum, P.J., Reinhardt, E.G., Beddows, P.A., Gabriel, J.J., 2010. Investigating linkages between Holocene paleoclimate and paleohydrogeology preserved in a Yucatan underwater cave. Quat. Sci. Rev. 29, 2788–2798.

van Hengstum, P.J., Scott, D.B., Gröcke, D.R., Charette, M.A., 2011. Sea level controls sedimentation and environments in coastal caves and sinkholes. Mar. Geol. 286, 35–50.

van Hengstum, P.J., Donnelly, J.P., Toomey, M.R., Albury, N.A., Lane, P., Kakuk, B., 2014. Heightened hurricane activity on the Little Bahama Bank from 1350 to 1650 AD. Cont. Shelf Res. 86, 103–115.

van Hengstum, P.J., Donnelly, J.P., Fall, P.L., Toomey, M.R., Albury, N.A., Kakuk, B., 2016. The intertropical convergence zone modulates intense hurricane strikes on the western North Atlantic margin. Sci. Rep. 6, 21728.

van Hengstum, P.J., Maale, G., Donnelly, J.P., Albury, N.A., Onac, B.P., Sullivan, R.M., Winkler, T.S., Tamalavage, A.E., MacDonald, D., 2018. Drought in the northern Bahamas from 3300 to 2500 years ago. Quat. Sci. Rev. 186, 169–185.

Hibbert, F.D., Williams, F.H., Fallon, S.J., Rohling, E.J., 2018. A database of biological and geomorphological sea level markers from the Last Glacial Maximum to present. Scientific Data 5, 180088.

Hine, A.C., Steinmetz, J.C., 1984. Cal Sal Bank, Bahamas: a partially drowned carbonate platform. Mar. Geol. 59, 135–164.

Holding, S., Allen, D.M., 2015. Wave overwash impact on small islands: generalised observations of freshwater lens response and recovery for multiple hydrogeological settings. J. Hydrol. 529, 1324–1335.

Holmes, J.A., 1997. Recent non-marine ostracoda from Jamaica, West Indies. J. Micropalaeontol. 16, 137–143.

Holmes, J.A., 1998. A late Quaternary ostracod record from Wallywash Great Pond, a Jamaican marl lake. J. Paleolimnol. 19, 115–128.

Hua, Q., Barbetti, M., 2004. Review of tropospheric Bomb ^{14}C data for carbon cycle modelling and age calibration purposes. Radiocarbon 46, 1273–1298.

Jury, M., Malmgren, B.A., Winter, A., 2007. Subregional precipitation climate of the Caribbean and relationships with ENSO and NAO. J. Geophys. Res. 112, D16107.

Kaldi, J., Gidman, J., 1982. Early diagenetic dolomite cements: examples from the Permian Lower Magnesian Limestone of England and the Pleistocene carbonates of The Bahamas. J. Sediment. Petrol. 52, 1073–1085.

Keyser, D., 1977. Ecology of zoogeography of recent brackish-water ostracods (crustacea) from south-west Florida. In: Löffler, H., Danielopol, D. (Eds.), Aspects of the Ecology and Zoogeography of Recent and Fossil Ostracoda. Dr. W. Junk Publishers, The Hague, pp. 207–222.

Khan, N.S., Ashe, E., Horton, B.P., Dutton, A., Kopp, R.E., Brocard, G., Engelhart, S.E., Hill, D.F., Peltier, W.R., Vane, C.H., Scatena, F.N., 2017. Drivers of Holocene sea-level change in the Caribbean. Quat. Sci. Rev. 155, 13–36.

Kindler, P., Hearty, P.J., 1997. Geology of the Bahamas: architecture of Bahamian Islands. In: Vacher, H.L., Quinn, T.M. (Eds.), Geology and Hydrogeology of Carbonate Islands. Elsevier, Amsterdam, pp. 141–160.

Kovacs, S.E., van Hengstum, P.J., Reinhardt, E.G., Donnelly, J.P., Albury, N.A., 2013. Late Holocene sedimentation and hydrologic development in a shallow coastal sinkhole on Great Abaco Island, the Bahamas. Quat. Int. 317, 118–132.

Kovacs, S.E., Reinhardt, E.G., Stastna, M., Coutino, A., Werner, C., Collins, S.V., Devos, F., Le Maillot, C., 2017. Hurricane Ingrid and Tropical Storm Hanna's effects on the salinity of the coastal aquifer, Quintana Roo, Mexico. J. Hydrol. 551, 703–714.

Koyama, T., 1976. A new species of *Torulinium* from the Bahama islands. Brittonia 28, 252–254.

Lane, P., Donnelly, J.P., Woodruff, J.D., Hawkes, A.D., 2011. A decadally-resolved paleohurricane record archived in the late Holocene sediments of a Florida sinkhole. Mar. Geol. 287, 14–30.

Loeblich Jr., A.R., Tappan, H., 1987. Foraminiferal Genera and their Classification. Van Nostrand Reinhold Company, New York.

Mackinnon, L., Jones, B., 2001. Sedimentological evolution of North Sound, Grand Cayman-a freshwater to marine carbonate succession driven by Holocene sea-level rise. J. Sediment. Res. 71, 568–580.

Maloof, A.C., Grotzinger, J.P., 2012. The Holocene shallowing-upward parasequence of north-west Andros Island, Bahamas. Sedimentology 59, 1375–1407.

Martin, J.B., Spellman, P., Gulley, J., 2010. Tidal pumping of freshwater-saltwater mixing in Bahamian Blue Holes. GSA Abstracts with Programs 42, 330.

Martin, J.B., Gulley, J., Spellman, P., 2012. Tidal pumping of water between Bahamian blue holes, aquifers, and the ocean. J. Hydrol. 416–417, 28–38.

Melim, L., Masaferro, J.L., 1997. Geology of the Bahamas: subsurface geology of the Bahamas banks. In: Vacher, H.L., Quinn, T.M. (Eds.), Geology and Hydrogeology of Carbonate Islands. Elsevier, Amsterdam, pp. 161–182.

Milne, G.A., Peros, M., 2013. Data-model comparison of Holocene sea-level change in the circum-Caribbean region. Glob. Planet. Chang. 107, 119–131.

Mylroie, J.E., Carew, J.L., Moore, A.I., 1995. Blue holes: definitions and genesis. Carbonates Evaporites 10, 225–233.

Neumann, A.C., Land, L.S., 1975. Lime mud deposition and calcareous algae in the bight of Abaco, Bahamas. J. Sediment. Petrol. 45, 763–786.

Pearse, A.S., Creaser, E.P., Hall, F.G., 1936. The Cenotes of the Yucatan: A Zoological and Hydrographic Survey. Carnegie Institution of Washington (304 pp).

Pérez, L., Lorenschat, J., Brenner, M., Scharf, B., Schwalb, A., 2010. Extant freshwater ostracodes (Crustacea: Ostracoda) from Lago Petén Itzá, Guatemala. International Journal of Tropical Biology 58, 871–895.

Perkins, R.D., Enos, P., 1968. Hurricane Betsy in the Florida-Bahama area: geologic effects and comparison with hurricane Donna. The Journal of Geology 76, 710–717.

Peros, M., Collins, S., Agosta G'Meiner, A., Reinhardt, E., Pupo, F.M., 2017. Multistage 8.2 kyr event revealed through high-resolution XRF core scanning of Cuban sinkhole sediments. Geophys. Res. Lett. 44, 7374–7381.

Pilarczyk, J.E., Dura, T., Horton, B.J., Englehard, S.E., Kemp, A.C., Sawai, Y., 2014.

Microfossils from coastal environments as indicators of paleo-earthquakes, tsunamis and storms. Palaeogeogr. Palaeoclimatol. Palaeoecol. 413, 144–157.

Pilskan, C.H., Neumann, A.C., Bane, J.M., 1989. Periplatform carbonate flux in the northern Bahamas. Deep-Sea Res. 36, 1391–1406.

Rankey, E.C., Enos, P., Steffen, K., Druke, D., 2004. Lack of impact of Hurricane Michelle on tidal flats, Andros Island. J. Sed. Res. 74 (5), 654–661.

Rasmussen, K.A., Haddad, R.I., Neuman, A.C., 1990. Stable-isotope record of organic carbon from an evolving carbonate banktop, Bight of Abaco, Bahamas. Geology 18, 790–794.

Reeder, S.L., Rankey, E.C., 2009. Controls on morphology and sedimentology of carbonate tidal deltas, Abacos, Bahamas. Mar. Geol. 267, 141–155.

Reeder, S.L., Rankey, E.C., 2012. A tale of two storms: an integrated field, remote sensing, and modeling study examining the impact of hurricanes Frances and Jeanne on carbonate systems, Bahamas. In: Swart, P.K., Eberly, G.P., McKenzie, J.A. (Eds.), Perspectives in Carbonate Geology: A Tribute to the Career of Robert Nathan Ginsberg. Wiley Blackwell, pp. 75–90.

Reimer, P.J., Bard, E., Bayliss, A., Beck, J.W., Blackwell, P.G., Bronk Ramsey, C., Buck, C.E., Cheng, H., Edwards, R.L., Friedrich, M., Grootes, P.M., Guilderson, T.P., Haflidason, H., Hajdas, I., Hatte, C., Heaton, T.J., Hoffman, D.L., Hogg, A.G., Hughen, K.A., Kaiser, K.F., Kromer, B., Manning, S.W., Niu, M., Reimer, R.W., Richards, D.A., Scott, E.M., Southon, J.R., Stafford, R.A., Turney, C.S.M., van der Plicht, J., 2013. IntCal 13 and Marine13 radiocarbon age calibration curves 0–50,000 years cal BP. Radiocarbon 55, 1869–1887.

Ritzi Jr., R.W., Bukowski, J.M., Carbey, C.K., Boardman, M.R., 2001. Explaining the thinness of the fresh water lens in the Pleistocene carbonate aquifer on Andros Island, Bahamas. Ground Water 39, 713–720.

Rose, P.R., Lidz, B.H., 1977. Diagnostic Foraminiferal Assemblages of Shallow-water Modern Environments: South Florida and the Bahamas. V. 6 Comparative Sedimentology Laboratory, Division of Marine Geology and Geophysics, Rosenstiel School of Marine & Atmospheric Science, University of Miami, Florida.

Sahoo, B., Jose, F., Bhaskaran, P.K., 2019. Hydrodynamic response of Bahamas archipelago to strom surge and hurricane generated waves - A case study for Hurricane Joaquin. Ocean Eng. 184, 227–238.

Sand-Jensen, K., Anderson, M.K., Martinsen, K.T., Borum, J., Kristensen, E., Kragh, T., 2019. Shallow plant-dominated lakes – extreme environmental variability, carbon cycling and ecological challenges. Ann. Bot. 124 (3), 355–366.

Schnurrenberger, D., Russell, J., Kelts, K., 2003. Classification of lacustrine sediments based on sedimentary components. J. Paleolimnol. 29, 141–154.

Sherman, K.D., Shultz, A.D., Dahlgren, C.P., Thomas, C., Brooks, E., Brooks, A., Brumbaugh, D.R., Gittens, L., Murchie, K.J., 2018. Contemporary and emerging fisheries in the Bahamas-conservation and management challenges, achievements, and future directions. Fish. Manag. Ecol. 25, 319–331.

Shinn, E.A., Lloyd, R.M., Ginsburg, R.N., 1969. Anatomy of a modern carbonate tidal-flat, Andros Island. Bahamas. Journal of Sedimentary Petrology 39, 1202–1228.

Shinn, E.A., Reich, C.D., Locker, S.D., Hine, A.C., 1996. A giant sediment trap in the Florida Keys. J. Coast. Res. 12, 953–959.

Slayton, I., 2010. A Vegetation History from Emerald Pond, Great Abaco Island, the Bahamas, Based on Pollen Analysis. Unpublished MSc Thesis. University of Tennessee, Knoxville, pp. 85.

Slowey, N., Henderson, G.M., 2011. Radiocarbon Ages Constraints on the Origin and Shedding of Bank Top Sediment in the Bahamas during the Holocene. Aquat. Geochem. 17, 419–429.

Soulié-Märsche, I., 2008. Charophytes, indicators for low salinity phases in North African

sebkhet. J. Afr. Earth Sci. 51, 69–76.

Soulié-Märsche, I., García, A., 2015. Gyrogonites and oospores, complementary viewpoints to improve the study of the charophytes (Charales). Aquat. Bot. 120, 7–17.

Steadman, D.W., Franz, R., Morgan, G.S., Albury, N.A., Kakuk, B., Broad, K., Franz, S.E., Tinker, K., Pateman, M.P., Lott, T.A., Jarzen, D.M., Dilcher, D.L., 2007. Exceptionally well preserved late Quaternary plant and vertebrate fossils from a blue hole on Abaco, the Bahamas. Proc. Natl. Acad. Sci. 104, 19897–19902.

Street-Perrott, F.A., Hales, P.E., Perrott, R.A., Fontes, J.C., Switsur, V.R., Pearson, A., 1993. Late Quaternary paleolimnology of a tropical marl lake: Wallywash Great Pond, Jamaica. J. Paleolimnol. 9, 3–22.

Surić, M., Juračić, M., Horvatinčić, N., Bronić, I.K., 2005. Late-Pleistocene-Holocene sea-level rise and the pattern of coastal karst inundation: records from submerged speleothems along the Eastern Adriatic Coast (Croatia). Mar. Geol. 214, 163–175.

Tamalavage, A.E., van Hengstum, P.J., Louchouarn, P., Molodtsov, S., Kaiser, K., Donnelly, J.P., Albury, N.A., Fall, P.L., 2018. Organic matter sources and lateral sedimentation in a Bahamian karst basin (sinkhole) over the late Holocene: Influence of local vegetation and climate. Palaeoclimatol. Palaeoecol. 506, 70–83. https://doi.org/10.1016/j.palaeo.2018.06.014.

Tedesco, L.P., Aller, R.C., 1997. ^{210}Pb Chronology of sequences affected by burrow excavation and infilling: examples from shallow marine carbonate sediment sequences, Holocene south Florida and Caicos Platform, British West Indies. J. Sediment. Petrol. 67, 36–46.

Teeter, J.W., 1980. Ostracoda of the Lake Flint Formation (Pleistocene) of Southern Florida. Micropaleontology 26, 337–355.

Teeter, J.W., 1989. Holocene salinity history of the saline lakes of San Salvador Island, Bahamas. In: Curran, H.A., Bain, R.J., Carew, J.L., Mylroie, J., Teeter, J.W., White, B. (Eds.), Pleistocene and Holocene Carbonate Evironments on San Salvador Island, Bahamas, San Salvador, the Bahamas, pp. 35–39.

Todd, R., Low, D., 1971. Foraminifera from the Bahama Bank West of Andros Island. US Geological Survey Professional Paper 683 − C (37 pp).

Vahrenkamp, V.C., Swart, P.K., 1994. Late Cenozoic dolomites of the Bahamas: metastable analogues for the genesis of ancient platform dolomites. In: Purser, B., Tucker, M., Zenger, D. (Eds.), Dolomites, a Volume in Honour of Dolomieu. International Association of Sedimentologists Special Publication 21. pp. 133–153.

Vahrenkamp, V.C., Swart, P.K., Ruiz, J., 1991. Episodic dolomitization of late Cenozoic carbonates in the Bahamas: evidence from strontium isotopes. J. Sediment. Petrol. 61, 1002–1014.

Wallace, E., Donnelly, J.P., van Hengstum, P.J., Wiman, C., Sullivan, R.M., Winkler, T.S., D'Entremont, N., Toomey, M.R., 2019. Intense hurricane activity over the past 1500 years at south Andros Island, the Bahamas. Paleoceanography and Paleoclimatology. https://doi.org/10.1029/2019PA003665.

Wanless, H.R., Tedesco, L.P., Tyrrell, K.M., 1987. Production of subtidal tubular and surficial tempestites by Hurricane Kate, Caicos Platform, British West Indies. J. Sediment. Petrol. 58 (4), 739–750.

Watts, W.A., Hansen, B.C.S., 1986. Holocene climate and vegetation of Bermuda. Pollen Spores 28, 355–364.

Weij, R., Reijmer, J.J.G., Eberlie, G.P., Swart, P.K., 2019. The limited link between accommodation space, sediment thickness, and inner platform facies distribution (Holocene-Pleistocene, Bahamas). The Depositional Record 21.

Whitaker, F.F., Smart, P.L., 1997. Hydrogeology of the Bahamian archipelago. In: Vacher, H.L., Quinn, T.M. (Eds.), Geology and Hydrogeology of Carbonate Islands. Elsevier, Amsterdam, pp. 183–216.